ARTICLES

Journal of Semiconductors
(2021) 42, 092601
doi: 10.1088/1674-4926/42/9/092601

A MXene-functionalized paper-based electrochemical immunosensor for label-free detection of cardiac troponin I

Li Wang[1], Yufeng Han[1], Hongchen Wang[1], Yaojie Han[1], Jinhua Liu[1, †], Gang Lu[1, †], and Haidong Yu[1, 2, †]

[1]Institute of Advanced Materials (IAM) & Key Laboratory of Flexible Electronics (KLoFE), Nanjing Tech University (NanjingTech), Nanjing 211816, China

[2]Frontiers Science Center for Flexible Electronics, Xi'an Institute of Flexible Electronics (IFE) and Xi'an Institute of Biomedical Materials & Engineering, Northwestern Polytechnical University, Xi'an 710072, China

Abstract: Convenient, rapid, and accurate detection of cardiac troponin I (cTnI) is crucial in early diagnosis of acute myocardial infarction (AMI). A paper-based electrochemical immunosensor is a promising choice in this field, because of the flexibility, porosity, and cost-efficacy of the paper. However, paper is poor in electronic conductivity and surface functionality. Herein, we report a paper-based electrochemical immunosensor for the label-free detection of cTnI with the working electrode modified by MXene (Ti_3C_2) nanosheets. In order to immobilize the bio-receptor (anti-cTnI) on the MXene-modified working electrode, the MXene nanosheets were functionalized by aminosilane, and the functionalized MXene was immobilized onto the surface of the working electrode through Nafion. The large surface area of the MXene nanosheets facilitates the immobilization of antibodies, and the excellent conductivity facilitates the electron transfer between the electrochemical species and the underlying electrode surface. As a result, the paper-based immunosensor could detect cTnI within a wide range of 5–100 ng/mL with a detection limit of 0.58 ng/mL. The immunosensor also shows outstanding selectivity and good repeatability. Our MXene-modified paper-based electrochemical immunosensor enables fast and sensitive detection of cTnI, which may be used in real-time and cost-efficient monitoring of AMI diseases in clinics.

Key words: paper-based immunosensor; MXene; electrochemical detection; cardiac troponin I (cTnI)

Citation: L Wang, Y F Han, H C Wang, Y J Han, J H Liu, G Lu, and H D Yu, A MXene-functionalized paper-based electrochemical immunosensor for label-free detection of cardiac troponin I[J]. *J. Semicond.*, 2021, 42(9), 092601. http://doi.org/10.1088/1674-4926/42/9/092601

1. Introduction

Acute myocardial infarction (AMI) is one of the most life-threatening diseases[1]. Early diagnosis of AMI is crucial for successful treatment of patients. Cardiac troponin I (cTnI) is considered as the most specific and sensitive indicator for AMI diagnosis, because it exists only in heart tissue and its concentration is highly related to the development of AMI. The cTnI level in patients is around 10 ng/mL at the beginning of AMI, but it increases rapidly to 20–550 ng/mL shortly after 18 h[2]. Therefore, developing convenient, fast, and sensitive analytical methods for detecting cTnI is crucially important. Currently, many methods, including fluorescent immunoassay[3–5], chemiluminescent immunoassay[6, 7], and colorimetric immunoassay[8, 9], have been used for sensitive detection of cTnI. However, these analytical methods usually require large-scale instruments and complicated operation steps. These shortages limit the applications of these methods in rapid diagnosis of AMI. Therefore, it is still urgent to develop simple, fast, cost-efficient, and portable devices for sensitive detection of cTnI for early diagnosis of AMI.

Paper-based sensors have attracted tremendous attention from researchers since George Whitesides fabricated a low-cost, low-fluid consumption, and portable microfluidic paper-based glucose sensor in 2007[10]. Paper-based sensors are usually fabricated by patterning a paper sheet into hydrophilic or hydrophobic channels by using various techniques, such as photolithography[11], screen printing[12, 13], calendaring[14], and wax printing[15, 16]. These technologies are facile, fast, inexpensive, and efficient for the fabrication of paper-based sensors[17]. At present, the mechanisms employed in paper-based sensors mainly include fluorescence, colorimetric, electrochemistry, and chemiluminescence. For example, Jiao and coworkers have integrated a sandwich-type fluorescent immunoassay device with a three-dimensional vertical-flow paper-based device (3VPD) for the detection of multiple cancer biomarkers[11]. Paper-based electrochemical biosensors have been extensively used because of their rapid response (within a few minutes), high sensitivity/selectivity, wide detection range, easy operation, and low required sample volume[14, 15]. In paper-based electrochemical sensors, the screen-printed electrodes (SPEs) have been extensively employed, owing to their easy fabrication and low cost[10, 18]. However, sensors with SPEs usually have low sensitivity due to the poor electron transfer. To overcome this drawback, two-dimensional (2D) materials with high conductivity, high specific surface area, and excellent biocompatibility have been developed for modifying SPEs.

MXenes are emerging 2D transition metal carbide and nitride materials with the formula $M_{n+1}X_nT_x$[19–21], where M, X,

Correspondence to: J H Liu, iamjhliu@njtech.edu.cn; G Lu, iamglv@njtech.edu.cn; H D Yu, iamhdyu@njtech.edu.cn, iamhdyu@nwpu.edu.cn

Received 8 FEBRUARY 2021; Revised 19 APRIL 2021.

and T represent early transition metals, C or N, and surface functional groups (-O, -OH, -F), respectively. *n* is in the range of 1 to 3[22, 23]. Owing to their high electron mobility, large surface area, abundant catalytic sites, and high biocompatibility[24–26], MXenes have attracted great interest in various applications of catalysis[27, 28], biosensor[19, 29, 30], supercapacitors[31, 32], and lithium ion batteries[33–35].

In this work, a cost-efficient and portable paper-based electrochemical immunosensor was successfully constructed by wax printing and screen-printing. The MXene nanosheets were used not only for improving the conductivity of SPEs, but also for immobilizing a large number of antibodies. The paper-based immunosensor with MXene-modified SPEs (MXene/SPEs) exhibited high sensitivity and selectivity towards cTnI with a low limit of detection (LOD) of 0.58 ng/mL, as well as good repeatability. Our paper-based immunosensor demonstrates great potential in highly sensitive detection of cTnI, which has a broad application prospect in clinical AMI diagnosis.

2. Experimental

2.1. Chemicals

Whatman chromatography paper (No. 1) was acquired from Zhengcheng Experimental Instrument Co., Ltd (Shanghai). Bovine serum albumin (BSA), Tween-20, and ethanol (99.5%) were supplied by Macklin Biochemical Co., Ltd (Shanghai). Phosphate buffered saline (PBS, 0.01 mol/L, pH = 7.4) and the PBS solution doped with 0.05% Tween-20 (PBST) were both freshly prepared. Human heart-type cardiac troponin I (cTnI) and capture monoclonal antibodies (anti-cTnI) were acquired from Linc-Bio Science Co., Ltd (Shanghai). The commercialized ELISA kit used to detect cTnI was acquired from Enzyme-linked Biotechnology Co., Ltd (Shanghai). All chemicals used in this work are analytical grade and used directly.

2.2. Characterizations

The morphology of MXene sheets was characterized with a transmission electron microscopy (TEM, JEM-1400PLUS, JEOL, Japan). The X-ray diffraction (XRD) patterns were collected on an X-ray diffractometer (SmartLab 3, Rigaku, Japan) with Cu Kα radiation (λ = 1.5418 Å). The atomic force microscopy (AFM) was performed on Park XE-70 (Korea). The cyclic voltammetry (CV) and differential pulse voltammetry (DPV) were conducted on CHI630E (CH Instrument, China). PalmSens4 (PalmSens, Netherlands) was used to measure the electrochemical impedance spectroscopy (EIS).

2.3. Synthesis of Ti_3C_2-MXene

Briefly, an etching solution was obtained by mixing 1 g of LiF and 5 mL of DI water with 15 mL of 12 mol/L HCl. Then, 1 g Ti_3AlC_2 (MAX) was added slowly into the etching solution, which was stirred for 24 h to remove the aluminum (Al) layer. Afterward, the mixed suspension was transferred to a centrifuge tube, which was then centrifuged at 3500 rpm for five minutes. The centrifugal product was repeatedly washed with DI water until the pH of supernatant was ⩾6. Subsequently, the cleaned product was mixed with DI water again, followed by being sonicated for one hour. Finally, the Ti_3C_2 (MXene) nanosheets were collected by centrifugation at 3500 rpm for 5 min.

2.4. Silanization of MXene sheets

The (3-aminopropyl) triethoxysilane (APTES) was used for the functionalization of the as-prepared Ti_3C_2-MXene nanosheets. In detail, 1 mL of APTES was gradually added to the mixed suspension that contains 100 mg Ti_3C_2-MXene nanosheets and 50 mL ethanol, and the suspension was stirred (500 rpm) for 48 h at room temperature. For the removal of unbound APTES molecules, the resulting product was washed three times with a mixture of water and ethanol (1 : 1). Then, the resulting product was dried at 50 °C in a vacuum overnight to obtain the APTES-functionalized Ti_3C_2-MXene (f-Ti_3C_2-MXene), which was then finely pulverized into powder and then sonicated in a 0.1% Nafion solution in ethanol and DI water for one hour to obtain a 1 mg/mL suspension.

2.5. Fabrication of paper-based electrochemical immunosensor

The paper-based electrochemical sensor was fabricated in the following four steps as described by Wang and coworkers[36]. First, hydrophilic channels were designed through PowerPoint software. Second, the designed channel structures were patterned on the surface of Whatman paper by using the Xexro digital wax printer. The wax-patterned paper was baked at 110 °C for 5 min, allowing the wax to melt again and sweep into the paper. Third, three electrodes were fabricated by screen-printing. The working and counter electrodes were prepared by printing conductive carbon ink, and the reference electrode was prepared by printing Ag/AgCl ink. The screen-printing electrodes (SPEs) were baked at 80 °C for 15 min. Finally, these two layers of paper were integrated together with double-sided tape.

2.6. Modification of the immunosensor

The modified paper-based electrochemical sensor was prepared according to the process shown in Fig. 1. First, f-Ti_3C_2-MXene was coated on the surface of the SPE, followed by drying at room temperature. Then, 60 μg/mL anti-cTnI was dropped on the MXene-modified electrode and incubated for 30 min. Subsequently, 10 μL 1% BSA solution was dropped to minimize the non-specific adsorption by blocking the remaining active sites. Finally, the immunosensors were stored at 4 °C before usage.

2.7. Electrochemical measurements

The DPV measurement was performed in the range of –0.2 to 0.7 V, while the scan rate of CV was 50 mV/s. EIS experiments were performed in the frequency range of 0.1–10 000 Hz and AC amplitude of 5 mV. The electrochemical tests were performed in a mixed solution of 0.1 mol/L KCl and 0.005 mol/L $K_3[Fe(CN)_6]$. The electrochemical detection, selectivity, and repeatability tests were performed in a PBS buffer (0.01 mol/L, pH = 7.4) containing $K_3[Fe(CN)_6]$/$K_4[Fe(CN)_6]$ (0.005 mol/L) and KCl (0.1 mol/L).

3. Result and discussion

3.1. Characterization of MXene nanosheets

The Ti_3C_2-MXene was prepared by etching the Al layers in the MAX (M = metal, A = Al, X = C or N) precursor in a mixed solution of hydrochloride (HCl) and lithium fluoride (LiF). The obtained MXene nanosheets were well dispersed in

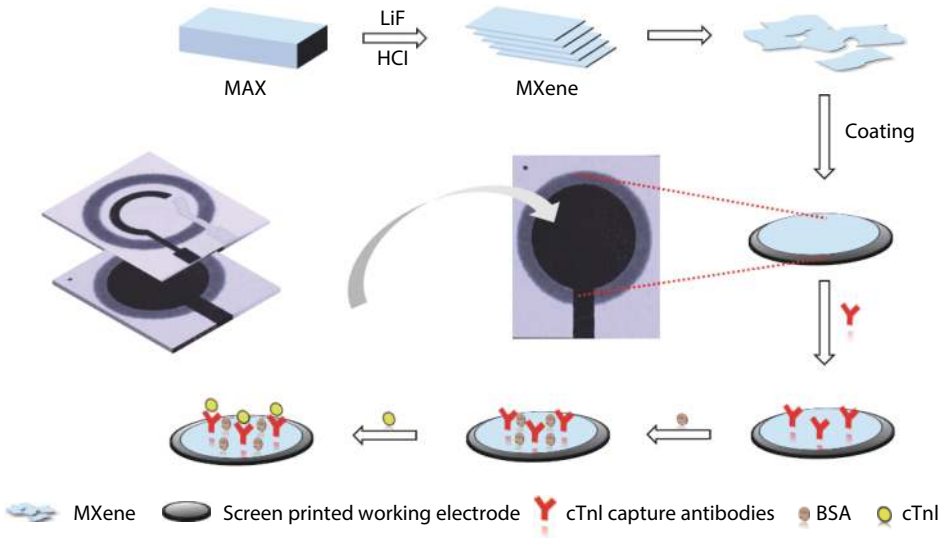

Fig. 1. (Color online) Schematic diagram illustrating the fabrication of the paper-based cTnI immunosensor and their usage in detection of cTnI.

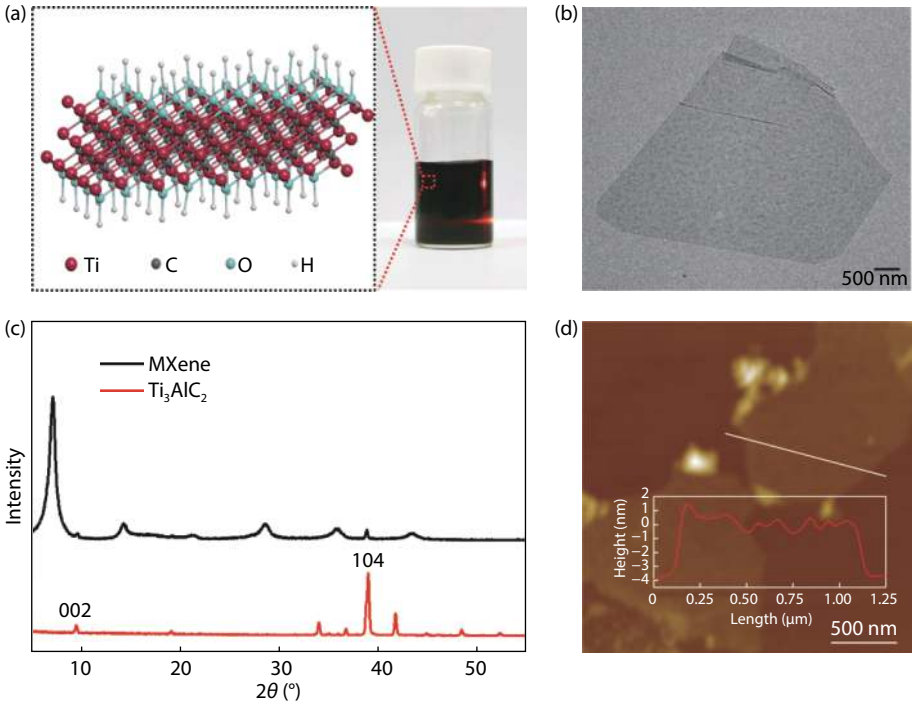

Fig. 2. (Color online) Characterizations of MXene. (a) Scheme showing the crystal structure of the MXene and a photograph of the colloid solution of the MXene. (b) TEM image of the MXene. (c) XRD patterns of the etched MXene (black line) and original MAX phase (red line). (d) AFM image of the Ti_3C_2 MXene. The insert is the line profile of the white line in (d).

aqueous solution, and the color of the suspension was dark green (Fig. 2(a)). The obtained Ti_3C_2-MXene nanosheet was thin and highly transparent to the electron beam in the TEM image (Fig. 2(b)). From the X-ray diffraction (XRD) pattern, the (104) peak of the MAX phase disappeared and the (002) peak left-shifted for 2.9 degrees (Fig. 2(c)), suggesting that the Ti_3C_2-MXene was successfully prepared. As shown in the atomic force microscopy (AFM) image (Fig. 2(d)), the thickness of the MXene nanosheets was only 4 nm, indicating that the obtained MXene nanosheets were only a few atomic layers thick. Moreover, the Fourier transform infrared (FT-IR) spectra of the pristine MXene and f-MXene (Fig. S1) were compared to investigate the salinization of Ti_3C_2-MXene with APTES. The bands at 567 and 1633 cm^{-1} were presented in the Ti_3C_2-MXene sample, and these two bands are ascribed to the vibration modes of the Ti–O and C=O bonds[25]. In the salinized MXene sample, the characteristic peaks of APTES were observed at 1100, 1618, 2942, and 2885 cm^{-1}, indicating the successful salinization of Ti_3C_2 MXene[37, 38].

3.2. Electrochemical characteristics of the modified electrodes

The synthesized MXene sheets were functionalized with APTES and then adsorbed on the paper-based SPEs. The interfacial properties of the modified electrodes were characterized by EIS. The impedance spectrum comprises a semicircular and a linear portion. The semicircular diameter at high frequency corresponds to the value of the charge transfer resist-

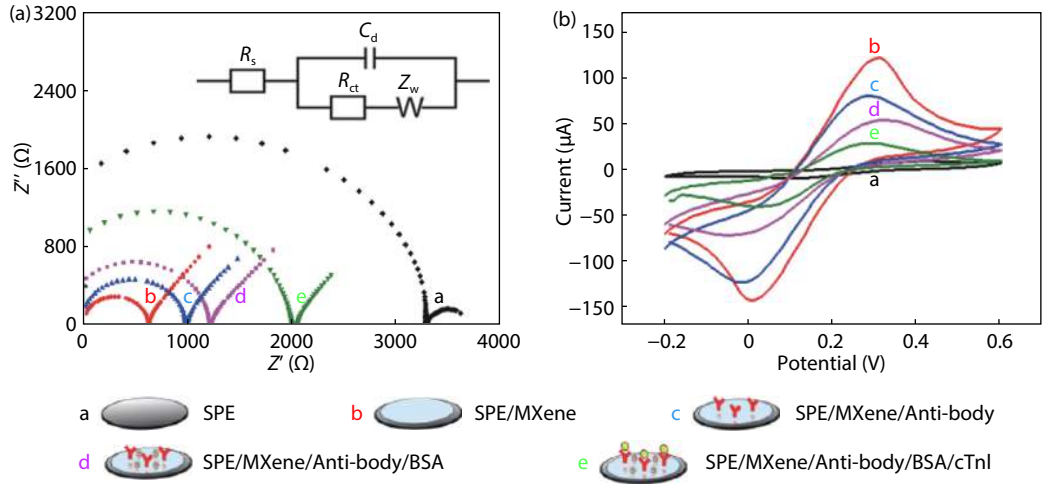

Fig. 3. (Color online) Surface modifications of the electrodes. (a) EIS of the modified electrodes measured in a mixed solution of KCl (0.1 mol/L) and $K_3[Fe(CN)_6]$ (0.005 mol/L). (b) CV of the modified electrodes, measured at a scan rate of 50 mV/s in a mixed solution of KCl (0.1 mol/L) and $K_3[Fe(CN)_6]$ (0.005 mol/L).

ance (R_{ct}), while the slope of the linear part at low frequency corresponds to the value of the diffusion resistance[39]. The changes of R_{ct} in the modified electrodes were monitored to illustrate the adsorption of the antibody. Fig. 3(a) shows the characteristic EIS spectra corresponding to the sequential modification of the electrodes. Compared with that of pure SPEs, the impedance spectra of the MXene/SPEs showed a much smaller semicircle radius, suggesting that the excellent conductivity of MXene nanosheets is beneficial to the electron transfer between the electrolyte and the interface. The R_{ct} value increased after modification of the f-MXene/SPEs surface with capture antibodies. The formation of the antibody layer on the f-MXene/SPE impedes the electron transfer between the redox probe ($[Fe(CN)_6]^{3-/4-}$) and electrode surface. Then, the R_{ct} was further increased after the modification with bovine serum albumin (BSA). A significant increase in R_{ct} was noticed after the bounding of target cTnI onto the capture antibody-modified f-MXene/SPEs, suggesting that the anti-cTnI and target cTnI have bonded successfully on the electrode surface. *C–V* curves of the different biomolecule-modified electrodes were also acquired. Fig. 3(b) shows that the peak current gradually decreases with the layer-by-layer modification of the electrode, which is consistent with the results of EIS. These results demonstrate a successful modification of the SPEs in the paper-based immunosensor.

3.3. Optimization of the immunoassay

To achieve the best analytical performance, the fabrication of the MXene-modified paper-based electrochemical immunosensor was optimized by tuning the pH value, antibody immobilization period, and PBST washing times. The pH value of buffer influences the properties of a biosensor greatly, due to the fact that the antibody may be inactivated in acidic or alkaline conditions[40]. The pH value of the buffer was chosen in the range of 5.5 to 9, and the electrochemical detections were performed. Optimal current response was obtained at pH value of 7.4 (Fig. 4(a)). Therefore, the subsequent tests were performed in PBS with a pH value of 7.4. Besides, the appropriate antibody immobilization period is of great importance, since a short immobilization period will increase many unspecific sites, which will cause an undesired background, while a long immobilization period will increase the detection time. The peak current evidently decreased with the increase of immobilization period from 10 to 30 min (Fig. 4(b)). After 30 min of antibody immobilization, the peak current tended to become flat. Therefore, 30 min was the optimal antibody immobilization period. PBST washing times will affect the sensing accuracy of the cTnI sensor. The excess biological samples may be attached to the working electrode via physical adsorption, which may interfere with the highly selective cTnI sensing. Therefore, the excess biological samples need to be removed by multiple washing. Within three times of washing, the change of peak current during sensing decreased, implying the unspecific binding of antibodies on the working electrode. However, with the washing times further increased, the peak current almost remained unchanged (Fig. 4(c)). Hence, three times was considered as the optimal PBST washing time.

3.4. Electrochemical detection of cTnI

In optimal conditions, the obtained immunosensor was used for the detection of cTnI at different concentrations, and the results were evaluated by DPV. The intensity of the peak DPV current decreased linearly with the increase in cTnI concentration within the range of 5–100 ng/mL, and a low LOD of 0.58 ng/mL was observed (Fig. 5(a)), which is due to the fact that the antibody layer forms a barrier layer on the electrode, impeding the electron transfer between the redox probe ($[Fe(CN)6]^{3-/4-}$) and electrode surface. Hence, cTnI could be quantitatively detected by monitoring the degree of the decreased peak DPV current. The linear regression equation was $y = -0.06876x + 31.49$ ($R^2 = 0.9745$), where y is the peak DPV current and x is the concentration of cTnI. Moreover, compared with other cTnI biosensors from Table 1, the obtained immunosensor can achieve a relatively lower detection limit, suggesting that the obtained paper-based electrochemical cTnI immunosensor has great application potential for measuring the cTnI in clinical diagnosis.

As a product made of natural materials, paper has been commonly used in portable and disposable devices, owing to

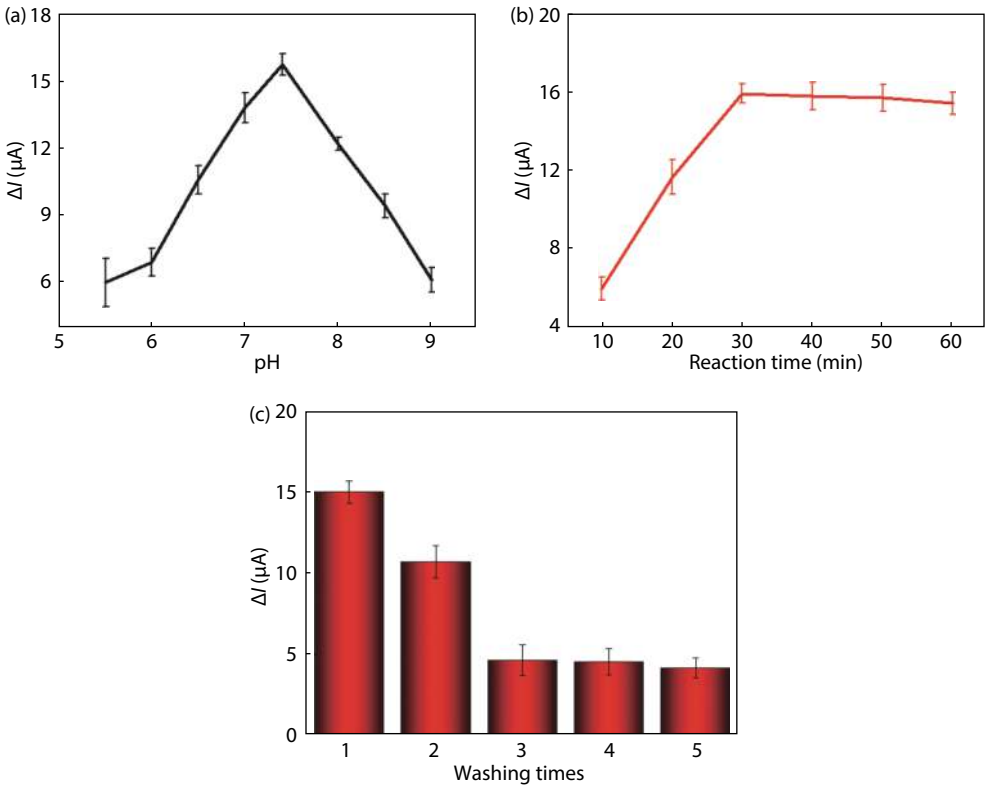

Fig. 4. (Color online) Optimization of the immunosensor. (a) The effect of pH value of PBS (5.5, 6, 6.5, 7, 7.4, 8, 8.5, and 9) on the current response of the immunosensor. (b) The effect of the immobilization period (10, 20, 30, 40, 50, and 60 min) of antibodies on the current response of the immunosensor, error bar = standard deviation (n = 5). (c) The effect of the washing times (1, 2, 3, 4, and 5) on the current response of the immunosensor.

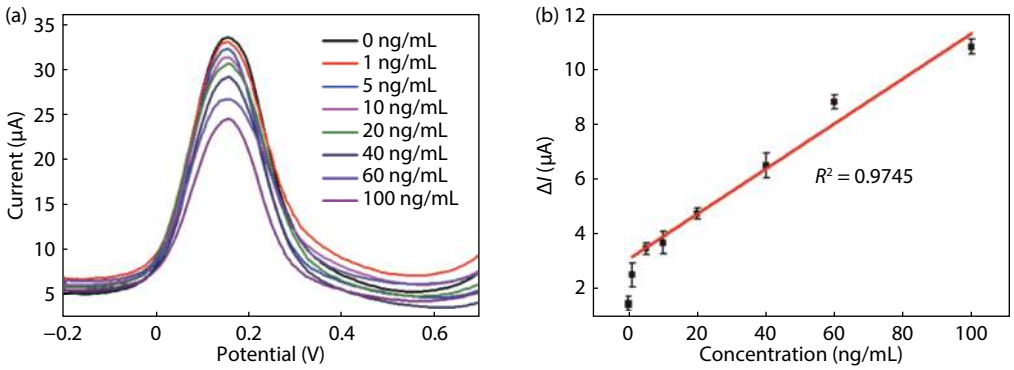

Fig. 5. (Color online) Electrochemical detection of cTnI. (a) DPV responses of the immunosensor to cTnI at concentrations of 0–100 ng/mL. (b) Calibration curve toward different concentrations of cTnI, error bar = standard deviation (n = 7).

Table 1. Performance comparisons of different cTnI biosensors.

Method	Sensing system	Sample	Linear range (ng/mL)	LOD (ng/mL)	Ref.
Fluorimetry	g-C_3N_4 QDs	PBS	10–1000	413	[41]
Fluorimetry	Aptamer	PBS		5	[42]
Colorimetric immunoassay	Anti-cTnI/HRP	Plasma	2.4–2400	5.6	[43]
Electrochemistry	Anti-cTnI/f-MXene	PBS	5–100	0.58	This work

g-C_3N_4 QDs: graphitic carbon nitride quantum dots. DDAB: didodecyldimethylammonium bromide.

its intrinsic flexibility, abundance, and low cost[44]. In addition, paper possesses a large specific surface area and excellent capillary effect due to the fiber-like microstructure of paper[45]. Therefore, the paper substrate with a unique porous structure and high absorptivity endows our paper-based immunosensor with high performance at a low cost.

3.5. Selectivity and repeatability of the immunosensor

Selectivity is a key factor to ensure the accuracy of biosensing. To estimate the selectivity of our paper-based immunosensor to cTnI, non-specific proteins (50 ng/mL) including bovine serum albumin (BSA), glucose oxidase (GOx), immuno-

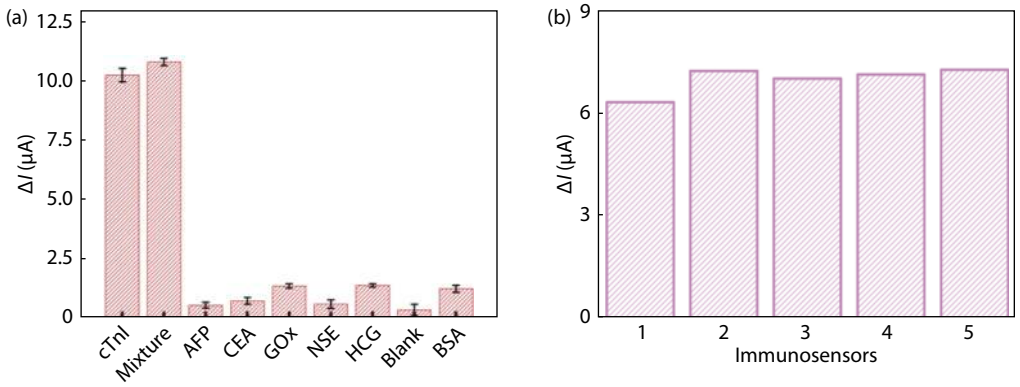

Fig. 6. (Color online) Characterization of the repeatability and selectivity of the immunosensor. (a) The selectivity to cTnI against non-target protein molecules: BSA, AFP, CEA, GOx, NSE, HCG, and Blank. (b) Reproducibility of the proposed immunosensors in the detection of cTnI.

globulins G (IgG), α-fetoprotein (AFP), carcinoembryonic antigen (CEA), neuron-specific enolase (NSE), human chorionic gonadotropin (HCG), and the mixed solution (including cTnI and these non-specific proteins) were tested for control studies. Fig. 6(a) shows that a marked decrease in peak current was found only in the cTnI solution and the mixed solution containing cTnI, indicating that the developed immunosensor has a high selectivity toward cTnI. Additionally, the reproducibility of our immunosensor was further estimated. Five paper-based immunosensors prepared with the same parameters were used to detect 50 ng/mL cTnI by DPV in the same optimal conditions. Fig. 6(b) shows that the obtained relative standard deviation (RSD) was only 6.3%, suggesting a high reproducibility of our immunosensor.

4. Conclusion

In summary, a label-free, highly sensitive and selective paper-based electrochemical immunosensor was successfully fabricated by functionalizing SPEs with two-dimensional Ti_3C_2-MXene nanosheets. The f-MXene nanosheets improve the conductivity of the SPEs greatly and also facilitate the immobilization of antibodies. Therefore, the sensitivity of the sensor was largely improved. The immunosensor exhibited high sensitivity and selectivity towards cTnI within the range of 5–100 ng/mL. A low LOD of 0.58 ng/mL was achieved. Moreover, the sensor also showed high repeatability. Owing to the advantages of low cost, fast response, high selectivity and sensitivity, our MXene-functionalized paper-based immunosensor demonstrates a great potential in label-free determination of cTnI in clinical diagnosis. Moreover, the inexpensive and environment-friendly nature of paper, as well as the simple fabrication procedure, make our paper-based immunosensor a promising candidate for green and flexible next-generation electronics.

Acknowledgements

This work was financially supported by the National Key R&D Program of China (2017YFA0204700), the Joint Research Funds of Department of Science & Technology of Shaanxi Province and Northwestern Polytechnical University (2020GXLH-Z-021), the China–Sweden Joint Mobility Project (51811530018), and the Fundamental Research Funds for the Central Universities.

Appendix A. Supplementary materials

Supplementary materials to this article can be found online at https://doi.org/1674-4926/42/9/092601.

References

[1] Mohammed M I, Desmulliez M P Y. Lab-on-a-chip based immunosensor principles and technologies for the detection of cardiac biomarkers: a review. Lab Chip, 2011, 11(4), 569

[2] Ko S, Kim B, Jo S S, et al. Electrochemical detection of cardiac troponin I using a microchip with the surface-functionalized poly(dimethylsiloxane) channel. Biosens Bioelectron, 2007, 23(1), 51

[3] Guo X Y, Zong L J, Jiao Y C, et al. Signal-enhanced detection of multiplexed cardiac biomarkers by a paper-based fluorogenic immunodevice integrated with zinc oxide nanowires. Anal Chem, 2019, 91(14), 9300

[4] Zhang C, Du P F, Jiang Z J, et al. A simple and sensitive competitive bio-barcode immunoassay for triazophos based on multi-modified gold nanoparticles and fluorescent signal amplification. Anal Chim Acta, 2018, 999, 123

[5] Kim H J, Shelver W L, Hwang E C, et al. Automated flow fluorescent immunoassay for part per trillion detection of the neonicotinoid insecticide thiamethoxam. Anal Chim Acta, 2006, 571(1), 66

[6] Wang M H, Liu J J, Qin X L, et al. Electrochemiluminescence detection of cardiac troponin I based on Au-Ag alloy nanourchins. Analyst, 2020, 145(3), 873

[7] Yang Z J, Shen J, Li J, et al. An ultrasensitive streptavidin-functionalized carbon nanotubes platform for chemiluminescent immunoassay. Anal Chim Acta, 2013, 774, 85

[8] Zhao Y J, Liu X H, Li J, et al. Microfluidic chip-based silver nanoparticles aptasensor for colorimetric detection of thrombin. Talanta, 2016, 150, 81

[9] Gao L, Yang Q F, Wu P. Recent advances in nanomaterial-enhanced enzyme-linked immunosorbent assays. Analyst, 2020, 145(12), 4069

[10] Martinez A W, Phillips S T, Butte M J, et al. Patterned paper as a platform for inexpensive, low-Volume, portable bioassays. Angew Chem Int Ed, 2007, 46(8), 1318

[11] Jiao Y C, Du C, Zong L J, et al. 3D vertical-flow paper-based device for simultaneous detection of multiple cancer biomarkers by fluorescent immunoassay. Sens Actuators B, 2020, 306, 127239

[12] Nair R R. Organic electrochemical transistor on paper for the detection of halide anions in biological analytes. Flex Print Electron, 2020, 5(4), 045004

[13] Yuan W, Wu X Z, Gu W B, et al. Printed stretchable circuit on soft elastic substrate for wearable application. J Semicond, 2018, 39(1), 015002

[14] Zong L J, Jiao Y C, Guo X Y, et al. Paper-based fluorescent immun-

oassay for highly sensitive and selective detection of norfloxacin in milk at picogram level. Talanta, 2019, 195, 333
[15] Zong L J, Han Y F, Gao L, et al. A transparent paper-based platform for multiplexed bioassays by wavelength-dependent absorbance/transmittance. Analyst, 2019, 144(24), 7157
[16] Wang D R, Mei Y F, Huang G S. Printable inorganic nanomaterials for flexible transparent electrodes: from synthesis to application. J Semicond, 2018, 39(1), 011002
[17] Li Z Y, Huang X, Lu G. Recent developments of flexible and transparent SERS substrates. J Mater Chem C, 2020, 8(12), 3956
[18] Zou M Z, Ma Y, Yuan X, et al. Flexible devices: from materials, architectures to applications. J Semicond, 2018, 39(1), 011010
[19] Wang H, Li H, Huang Y, et al. A label-free electrochemical biosensor for highly sensitive detection of gliotoxin based on DNA nanostructure/MXene nanocomplexes. Biosens Bioelectron, 2019, 142, 111531
[20] Naguib M, Kurtoglu M, Presser V, et al. Two-dimensional nanocrystals produced by exfoliation of Ti_3AlC_2. Adv Mater, 2011, 23(37), 4248
[21] Ren Z H, Qi D C, Sonar P, et al. Flexible sensors based on hybrid materials. J Semicond, 2020, 41(4), 040402
[22] Naguib M, Mochalin V N, Barsoum M W, et al. 25th anniversary article: MXenes: a new family of two-dimensional materials. Adv Mater, 2014, 26(7), 992
[23] Naguib M, Mashtalir O, Carle J, et al. Two-dimensional transition metal carbides. ACS Nano, 2012, 6(2), 1322
[24] Neupane G P, Yildirim T, Zhang L L, et al. Emerging 2D MXene/organic heterostructures for future nanodevices. Adv Funct Mater, 2020, 30(52), 2005238
[25] Xiao R, Zhao C X, Zou Z Y, et al. In situ fabrication of 1D CdS nanorod/2D Ti_3C_2 MXene nanosheet Schottky heterojunction toward enhanced photocatalytic hydrogen evolution. Appl Catal B, 2020, 268, 118382
[26] Meng Y, Ho J C. MXene-based wearable biosensor. J Semicond, 2019, 40(11), 110202
[27] Li Z, Wu Y. 2D early transition metal carbides (MXenes) for catalysis. Small, 2019, 15(29), 1804736
[28] Ahmed B, El Ghazaly A, Rosen J. i-MXenes for energy storage and catalysis. Adv Funct Mater, 2020, 30(47), 2000894
[29] Huang K, Li Z J, Lin J, et al. Two-dimensional transition metal carbides and nitrides (MXenes) for biomedical applications. Chem Soc Rev, 2018, 47(14), 5109
[30] Zhang H X, Wang Z H, Zhang Q X, et al. Ti_3C_2 MXenes nanosheets catalyzed highly efficient electrogenerated chemiluminescence biosensor for the detection of exosomes. Biosens Bioelectron, 2019, 124, 184
[31] Jiang Q, Kurra N, Alhabeb M, et al. All pseudocapacitive MXene-RuO_2 asymmetric supercapacitors. Adv Energy Mater, 2018, 8(13), 1703043
[32] Yang Q Y, Xu Z, Fang B, et al. MXene/graphene hybrid fibers for high performance flexible supercapacitors. J Mater Chem A, 2017, 5(42), 22113
[33] Du Y T, Kan X, Yang F, et al. MXene/graphene heterostructures as high-performance electrodes for Li-ion batteries. ACS Appl Mater Inter, 2018, 10(38), 32867
[34] Ahmed B, Anjum D H, Gogotsi Y, et al. Atomic layer deposition of SnO_2 on MXene for Li-ion battery anodes. Nano Energy, 2017, 34, 249
[35] Ahmed B, Anjum D H, Hedhili M N, et al. H_2O_2 assisted room temperature oxidation of Ti_2C MXene for Li-ion battery anodes. Nanoscale, 2016, 8(14), 7580
[36] Wang Y, Luo J P, Liu J T, et al. Electrochemical integrated paper-based immunosensor modified with multi-walled carbon nanotubes nanocomposites for point-of-care testing, of 17 beta-estradiol. Biosens Bioelectron, 2018, 107, 47
[37] Zhang G L, Wang T C, Xu Z H, et al. Synthesis of amino-functionalized $Ti_3C_2T_x$ MXene by alkalization-grafting modification for efficient lead adsorption. Chem Commun, 2020, 56, 11283
[38] White L D, Tripp C P. Reaction of (3-Aminopropyl)dimethylethoxysilane with amine catalysts on silica surfaces. J Colloid Interf Sci, 2000, 232, 400
[39] Lei J M, Chen X M. RuO_2/MnO_2 composite materials for high-performance supercapacitor electrodes. J Semicond, 2015, 36(8), 083006
[40] Wang S P, Wang J J, Zhu Y F, et al. Cantilever with immobilized antibody for liver cancer biomarker detection. J Semicond, 2014, 35(10), 104008
[41] Miao L Y, Jiao L, Tang Q R, et al. A nanozyme-linked immunosorbent assay for dual-modal colorimetric and ratiometric fluorescent detection of cardiac troponin I. Sens Actuators B, 2019, 288, 60
[42] Lee S, Kang S H. Quenching effect on gold nano-patterned cardiac troponin I chip by total internal reflection fluorescencemicroscopy. Talanta, 2013, 104, 32
[43] Torabi F, Mobini F H R, Danielsson B, et al. Development of a plasma panel test for detection of human myocardial. Biosens Bioelectron, 2007, 22, 1218
[44] Gong M M, Sinton D. Turning the page: advancing paper-based microfluidics for broad diagnostic application. Chem Rev, 2017, 117, 8447
[45] Noviana E, McCord C P, Clark K M, et al. Electrochemical paper-based devices: sensing approaches and progress toward practical applications. Lab Chip, 2019, 20, 9

Li Wang got her BS from Henan University of Science and Technology in 2019. Now she is a master's student under the supervision of Prof. Haidong Yu and Prof. Gang Lu in the Institute of Advanced Materials at Nanjing Tech University. Her research focuses on organic thin-film transistors, chemical and biological sensors.

Jinhua Liu received his PhD degree under the supervision of Prof. Ronghua Yang at Hunan University in China in 2012, and then worked as a postdoc at the University of Hong Kong (HKU). He joined the Institute of Advanced Materials at Nanjing Tech University as an associate professor. His research focuses on biosensor and immunosensor based on fluorescent nanomaterials.

Gang Lu received his PhD degree in Prof. Hua Zhang's group at Nanyang Technological University in Singapore in 2012, and then worked as a postdoc at KU Leuven and UC Berkeley. Since 2016, he is a professor in the Institute of Advanced Materials at Nanjing Tech University. His research focuses on plasmon-enhanced spectroscopy and photochemistry, and sensitive detection of chemicals and biomolecules.

Haidong Yu received his BS in chemistry from Peking University and PhD in bioengineering from National University of Singapore. Then he worked as a postdoc at Whitesides research group at Harvard University. He joined the Institute of Advanced Materials at Nanjing Tech University in 2015. He is now a professor at the Institute of Flexible Electronics at Northwestern Polytechnical University. His research focuses on green flexible electronics for healthcare applications.